Effect of Hybrid Machining Techniques on Machining Performance of In-House Developed Mg-PMMC

Navneet Khanna[1] · N. M. Suri[2] · Chetan Agrawal[1] · Prassan Shah[1] · Grzegorz M. Krolczyk[3]

Abstract High demand of lightweight material makes magnesium alloys and composites more suitable to aerospace and automotive industries. However, poor corrosion resistance and fatigue resistance make its applications limited. Due to inherent capability of machining processes, the surface characteristics of the component can be improved. Many articles reported improvement in machinability of different difficult-to-machine materials while using ultrasonic-assisted turning (UAT) process and cryogenic-assisted turning individually. In this paper, the newly developed cryogenic–ultrasonic-assisted turning (CUAT) technique is used for the machining of in-house developed magnesium AZ91/SiC particulate metal matrix composite (PMMC). In this study, surface roughness and chip breakability index are measured under different machining methods, i.e. conventional turning (CT), UAT and CUAT. The full factorial method is used to design the experiments. A regression model of surface roughness is developed for CT and UAT processes and optimized using Jaya algorithm. Our results provide evidence of improvement in surface finish for UAT of magnesium AZ91/SiC PMMC in comparison with CT. An improvement up to 36.50% and 15% has been observed in surface roughness and chip breakability index, respectively, with CUAT process as compared to UAT process at optimized cutting parameters of the UAT process.

List of Symbols

PMMC	Particulate metal matrix composite
UAT	Ultrasonic-assisted turning
CT	Conventional turning
CAT	Cryogenic-assisted turning
CUAT	Cryogenic–ultrasonic-assisted turning
C_{in}	Chip breakability index
N	Spindle speed in revolutions per minute (rpm)
f	Feed in mm per revolution
F	Frequency in kHz
R_a	Average surface roughness (μm)
R	Cutting tool nose radius (mm)

✉ Chetan Agrawal
  chetanagrawal@iitram.ac.in

1   Department of Mechanical Engineering, Institute of Infrastructure Technology Research and Management (IITRAM), Ahmedabad 380026, India

2   Department of Production and Industrial Engineering, Punjab Engineering College, Chandigarh 160012, India

3   Faculty of Mechanical Engineering, Opole University of Technology, Opole, Poland

1 Introduction

In the modern era, industries are striving to make lightweight components with superior functional performance and long product life to achieve sustainability in terms of economic and environmental aspects [1]. Stricter government regulations for environmental protection and global competition make industries to switch over to new materials and improved manufacturing methods to achieve higher productivity [2]. Magnesium alloy is one of the promising options that can be used as a light weight material in defence, automotive and aerospace industries.

The magnesium composites of AZ91 series find applications in the transmission casings, valve covers, intake manifolds, brackets, pumps, etc. [1–3]. It can also be used as a biodegradable material for medical implants [3]. But poor surface finish causes a high corrosion rate under saline medium which limits applications of magnesium alloys. It has been widely reported in the literature that good surface finish of machined components enhances its functional performance [4]. During machining, material goes under severe plastic deformation (SPD) due to very high magnitude of strains [up to 10] and strain rates [up to 10^6 s^{-1}] are involved. Refinement of grain occurs due to SPD, but it is limited due to generation of high temperature in cutting zone [5]. The surface roughness is dependent on grain refinement during machining process [6]. To address this issue, UAT and CUAT processes have been investigated in this study. Both of these approaches help to reduce the temperature generated in the cutting zone.

Generally in UAT process, vibration of resonance frequency 20–40 kHz and displacement amplitude of magnitude generally 10–15 μm is applied to the tool [7]. Vibration to the tool can be given in cutting or feed direction and/or in both the directions [8]. The essential purpose of this technique is to allow intermittent contact of tool-workpiece rather than continuous [9].

To produce superior machined surface, CAT process is emerging as a sustainable option due to its exceptional properties over other CM processes such as very low boiling point (− 196 °C for liquid nitrogen at 1 atm), non-toxicity and environmental friendliness [2, 10]. The CAT process consists of injecting a low-temperature fluid (liquid nitrogen or liquid CO_2) into the cutting zone. It dissipates heat quickly from cutting zone and reduces its temperature drastically. CAT process provides benefits over CT process in terms of improvement in surface roughness, reduction in tool wear while machining of different heat-resistant alloy [11].

Babitsky et al. [12] presented experimental and numerical analysis of surface roughness and roundness for Inconel 718 under UAT and CT processes. Results indicate an improvement of surface roughness and roundness up to 50% and increase of 50% in temperature under UAT process as compared to CT process.

Razfar et al. [13] carried out ultrasonic-assisted milling on AISI 1020 steel and compared surface roughness with conventional milling. Experimental data showed that surface roughness improved by 12.9% on an average. Ultrasonic assistance was more effective at low values of process parameters.

Pu et al. [14] investigated the effect of tool radius on surface integrity of AZ31B Mg alloy under dry and cryogenic machining. It was observed that surface roughness got reduced by 20% in cryogenic machining as compared

to dry machining irrespective of tool radius. It was shown that with large tool radius, compressive residual stress improved under cryogenic machining.

Outeiro et al. [15] developed a numerical model to predict cutting mechanics and surface integrity of AZ31B-O Mg alloy for different process parameters under dry and cryogenic machining. Results showed that thickness of affected layer increased and specific cutting energy got reduced as the value of feed increased.

Danish et al. [16] presented thermal analysis of AZ31B Mg alloy during cryogenic and dry turning process. Results showed up to a maximum of 57–60% reduction in temperature and 45–56% reduction in surface roughness under cryogenic machining as compared to dry turning process.

Shen et al. [17] worked on microstructure evolution of AZ31B Mg alloy during cryogenic machining using dislocation density-based constitutive material model. The obtained results revealed that surface integrity could be significantly improved during cryogenic machining.

Iorio et al. [18] utilized FEM to investigate vibration behaviour of horn and developed UAM set-up. This set-up was used to evaluate surface topography of commercially available AZ31B Mg alloy. The obtained results revealed that UAM could be an efficient option for machining of Mg alloys.

Mohammad et al. [19] used analytical approach to calculate the critical speed for ultrasonic-assisted milling operation. Here, the effect of cutting speed and vibrational amplitude was analysed. At higher cutting speed, effect of ultrasonic assistance was reduced. Higher amplitude vibration was more effective in ultrasonic milling operation.

The hybrid machining process was considered as a combination of two or more manufacturing processes. It was chosen to take advantages of combined processes. In recent years, the capability of both UAT process and CAT process is emerging individually to increase machinability of different materials. This paper aims to study the combined effect of these two processes on surface roughness and chip breakability index. This hybrid machining process can be termed as CUAT process. Although the influence of CT process on the surface roughness of different magnesium alloys is reported in available literature, UAT process and CUAT process of magnesium AZ91/SiC PMMC are still not reported in the available literature.

This novel research presents the following contributions. First, magnesium AZ91/SiC PMMC has been developed in-house as per the requirement of the automotive industry using a modified stir casting set-up. Second, the influence of UAT process of magnesium AZ91/SiC PMMC on cutting parameters suggested by the industry has been investigated in terms of surface roughness and chip breakability index and then compared with CT process. Third, the machining parameters are optimized using Jaya algorithm

Table 1 Composition of magnesium composite

Element	Al	Zn	SiC	Mg
Weight %	10	1	5	Remaining

Table 2 Composition of AZ91 alloy

Element	Al	Zn	Si	Mn	Fe	Cu	Ni	Mg
Weight %	9	1	0.035	0.035	0.005	0.0005	0.001	Remaining

Table 3 Detail of reinforcement in matrix alloy

Element	AZ91	SiC (200 mesh)
Weight %	95	5

for UAT process and CT process separately. Finally, the newly CUAT technique has been tested to machine the magnesium AZ91/SiC PMMC on optimized input parameters to investigate the effect on surface finish and chip breakability index.

This paper is organized as follows. The in-house development of the magnesium composite is presented in Sect. 2. The experimental set-up and methodology is presented in Sect. 3. Experimentation results of UAT and CT processes are presented in Sect. 4. The experimental data of Sect. 4 are used to develop the regression model, and its optimization using Jaya algorithm is carried out in Sect. 5. In Sect. 6, hybrid machining is performed on the optimized parameters obtained for UAT process. Finally, the conclusions are presented.

2 In-House Fabrication Process

In the present investigation, a modified stir casting set-up has been used in fabrication of magnesium AZ91/SiC PMMC. Magnesium AZ91 was used as base matrix, and SiC of 200 mesh size was used as the reinforcement phase in the development of magnesium metal matrix composite. The chemical composition of base alloy used in the present investigation is listed in Tables 1 and 2, respectively. Magnesium AZ91 alloy in 700 gm was poured in the air-tight mixing chamber. The required amount of Magnesium AZ91 was melted in the inert environment due to inflammable tendency of magnesium in open environment. The 4:1 ratio of SF_6 and argon (99.9% purity) was used in an inert environment during fabrication process. During fabrication process, the melting point of the alloy was observed to be 650 °C. A mechanical stirrer with 300 rpm stirring speed was used to get homogeneous mixture of added powder. The SiC (200 mesh size) particles with 5 wt% fraction were added as reinforcement into the vortex of the melt as listed in Table 3. The particles were preheated at 400 °C prior to addition into the melt vortex to eliminate moisture content. The required weight fraction of reinforced particles with controlled feed rate was added into the melt. The mixing of the reinforced particles into the vortex was

Fig. 1 Casting set-up used for fabrication of magnesium composite

done at 300 rpm through stirrer. The homogeneous mixture was then poured into the preheated mould through bottom gate in vacuum environment. The systematic set-up used in the present investigation is shown in Fig. 1.

2.1 Microstructure of Magnesium Composite

The cylindrical specimens of size 20 mm were prepared using the polishing machine. The microstructure was observed without etching agent. Microstructure analysis was performed by inverted metallurgical microscope, Carl Zeiss. Figures 2 and 3 are the images of microstructure at a magnification of 10X and 20X, respectively.

3 Experimental Set-up and Methodology

The subsections of experimental set-up and methodology are organized as follows. The first subsection describes the experimental set-up for performing CT and UAT processes. Second subsection presents design of experimental details. The methodology used for analysis which includes chip characterization method, regression model and Jaya algorithm is presented in subsection three.
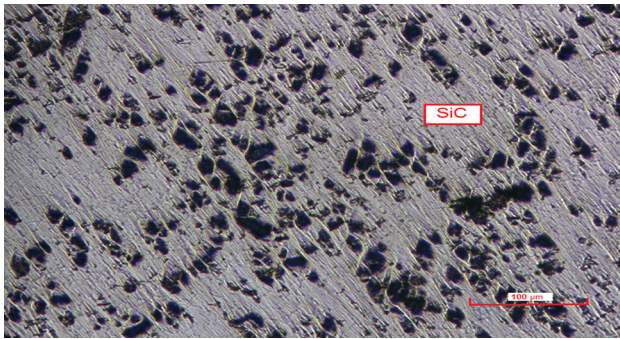
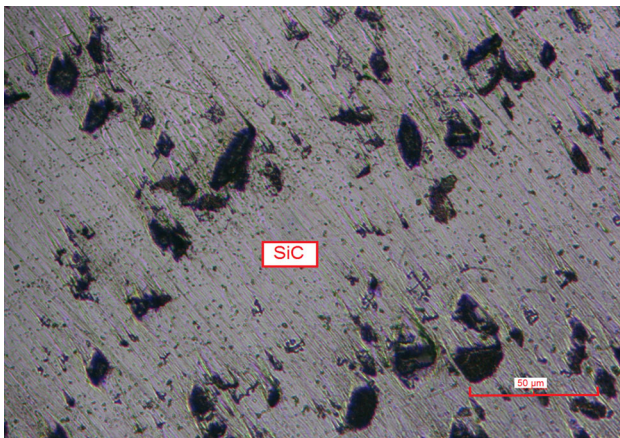**Fig. 2** The microstructure of AZ91 magnesium composite reinforced with 5 SiC at 10X

Fig. 3 The microstructure of AZ91 magnesium composite reinforced with 5 SiC at 20X

3.1 Experimental Set-up

The experimentation was carried out on a conventional lathe machine. The turning inserts selected were Kyocera TiAlN coating CNMG 120408CQ with rack angle of 7°. The workpiece of magnesium AZ91/SiC PMMC was used in the form of circular bar having dimension of diameter of 20 mm and length 180 mm. Taylor Hobson Sutronic S128 surface roughness tester was used to check the surface finish of workpiece. Mitutoyo toolmakers microscope attached with a camera was used to determine dimensions and shape of chip.

For UAT process, a system was developed to generate vibrations to the cutting tool in the cutting direction. The main components of the system were frequency generator, ultrasonic horn, piezoelectric transducer, high-frequency cable and fixture to hold ultrasonic horn. These components were assembled as shown in Fig. 4. A frequency generator was used to generate high-frequency and low-amplitude ultrasonic wave. A piezoelectric transducer which was mounted on an ultrasonic horn converted an

electrical signal supplied by frequency generator into mechanical vibration. Step horn was used to magnify amplitude of vibration up to 10–15 μm. In this experiment, ultrasonic vibration of frequency and amplitude of 20 kHz and 10 μm were applied, respectively, to the cutting tool. Equation (1) shows the necessary condition for choosing cutting speed range for UAT [9]. Here, V_c is cutting speed, a is the amplitude of vibration, and F is ultrasonic frequency applied.

$$V_c < 2\pi a F. \tag{1}$$

For CUAT process, conventional lathe was retrofitted with a combination of two set-ups, namely UAT process and CAT process as shown in Fig. 4. Cryogenic delivery system consisted of Dewar, vacuum jacketed hose and spray nozzle. The liquid nitrogen was stored at 1.5 MPa in Dewar which was fitted with a safety valve, liquid nitrogen level gauge, flow control valve and solenoid valve. A nozzle of 2 mm diameter sprayed the liquid nitrogen at rake face. Vacuum jacketed hose was used to transfer liquid nitrogen from Dewar to spray nozzle.

3.2 Design of Experiments

It is widely considered that design of experiments is an essential part to improve the process performance and product quality for metal cutting industries [20]. In this study, the full factorial experimental design was planned for optimization of process parameter for the machining of magnesium AZ91/SiC PMMC. Three levels of rotational speed (371, 557, 835 rpm), feed (0.111, 0.222, 0.333 mm/rev) and two level of frequency, i.e. 0 kHz (CT) and 20 kHz (UAT), were considered. Thus, as per the full factorial experimental design, the total number of experiments required to conduct were 18(3 × 3 × 2). A depth of cut of 0.2 mm was kept constant for all experiments. Each experiment shown in Table 4 replicated three times to minimize experimental noise. A fresh cutting edge was used for each replicates. Surface roughness, chip breakability index and types of chip produced were recorded as responses.

3.3 Methodology

This section describes the methods, namely chip characterization method, regression modelling and Jaya algorithm in subsequent subsections to analyse the responses like surface roughness and chip breakability index (C_{in}).

3.3.1 Chip Characterization Method

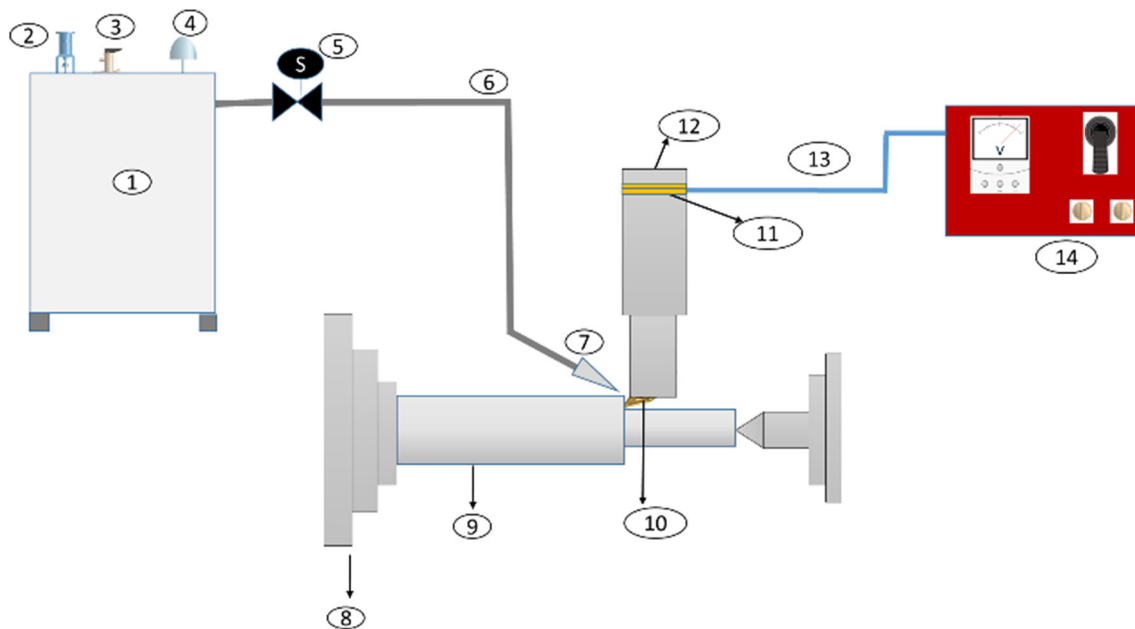One of the methods to characterize the chip breakability, produced in machining, is analyses of shape and size of

Fig. 4 Schematic of hybrid machining set-up: (1) liquid nitrogen source; (2) liquid nitrogen level gauge; (3) safety valve; (4) flow control valve; (5) solenoid valve; (6) vacuum insulated hose; (7) spray nozzle; (8) conventional lathe; (9) workpiece; (10) cutting insert; (11) piezoelectric transducer; (12) ultrasonic horn; (13) high-frequency cable; (14) frequency generator

Table 4 Experimental design based on full factorial

Experiment no.	N (rpm)	f (mm/rev)	F (kHz)	R_a (µm)	C_{in}	Types of chip produced
1	371	0.111	0	0.81	0.83	Helical
2	371	0.222	0	0.88	0.92	Arc
3	371	0.333	0	0.89	1.00	Arc
4	557	0.111	0	0.73	0.75	Helical
5	557	0.222	0	0.73	0.92	Arc
6	557	0.333	0	0.85	0.92	Arc
7	835	0.111	0	0.81	0.67	Snarled
8	835	0.222	0	0.78	0.92	Arc
9	835	0.333	0	0.93	0.67	Straight
10	371	0.111	20	0.63	0.75	Helical
11	371	0.222	20	0.71	0.83	Arc
12	371	0.333	20	0.75	0.67	Straight
13	557	0.111	20	0.74	0.81	Helical
14	557	0.222	20	0.80	0.92	Arc
15	557	0.333	20	0.70	0.67	Straight
16	835	0.111	20	0.66	0.83	Spiral
17	835	0.222	20	0.68	0.67	Straight
18	835	0.333	20	0.81	0.83	Straight

chip. Chip breakability index, C_{in}, is a parameter to analyse the chip which depends on shape and size of the chip produced. Its value lies between 0 and 1. A higher value of C_{in} denotes better chip breakability. According to the shape and size of the chip produced, they are classified into a different groups and this information is converted into a numerical value (C_{in}) using already established method [21, 22]. The expression for calculating chip breakability
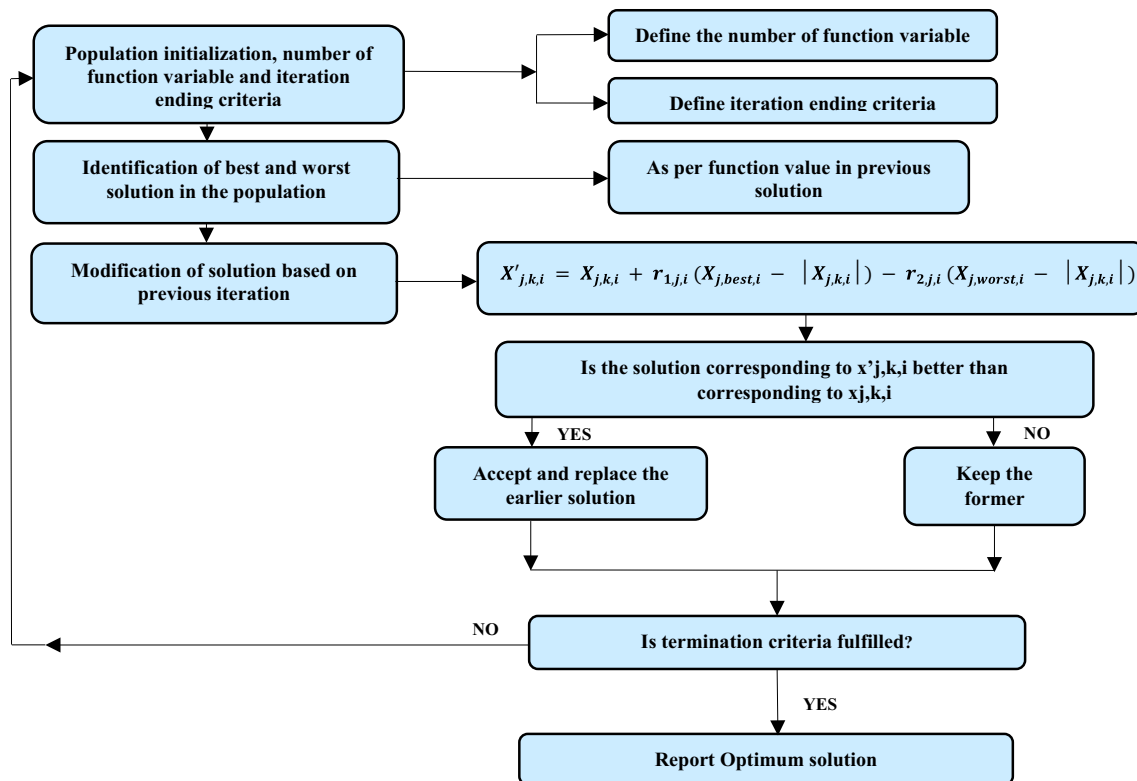
Fig. 5 A schematic representation of Jaya algorithm

index is shown in Eq. (2), where $\mu(A_k)$ is chip form grade fuzzy membership function which denotes the size and shape of the chip. The shape of the chip is classified into four different groups, namely arc, spiral/circular, helical and ribbon. Ribbon form is further sub-classified into straight, curled and snarled. Size of chip is classified into short, medium, large and very large. To convert the linguistic chip form grade to numerical value, $\omega(A_k)$ is defined in five different levels, i.e. excellent, good, fair, poor and very poor.

$$C_{in} = \frac{\sum_1^5 \mu(A_k) \cdot \omega(A_k)}{\sum_1^5 \mu(A_k)}. \tag{2}$$

3.3.2 Regression Model

Basic theoretical equation for surface roughness (R_a) is shown in Eq. (3), which depends on feed (f) and cutting tool nose radius (R). It does not account for any alteration or imperfection in the machining method such as ultrasonic-assisted vibration of the tool, the effect of cooling condition, etc., influencing the surface finish during machining. Elevated temperature during cutting process alters friction coefficient and tool edge condition. Therefore, regression model is developed in this investigation in order to accurately model the influence of ultrasonic assistance to the tool and other noise factors on surface

roughness. Equation (4) shows general mathematical expression for second-order regression model [23]. Regression model obtained for CT and UAT processes is optimized using Jaya algorithm individually.

$$R_a = \frac{f^2}{8R} \tag{3}$$

$$y = \beta_0 + \sum_{i=1}^{k} \beta_i x_i + \sum_{i=1}^{k} \sum_{j>1}^{k} \beta_i x_i x_j + \sum_{i=1}^{k} \beta_{ij} x_i^2. \tag{4}$$

3.3.3 Jaya Algorithm

Jaya algorithm was developed by [24]. This popular optimization method converges towards optimum solution by accepting the best value each time and eliminating the worst value. Flowchart of Jaya algorithm is shown in Fig. 5. In flowchart, expression showing $x'jki$ and $xjki$ represents modified new and old value of optimizing function. xj best i and xj worst i represent the best value and worst value of optimizing value at a particular iteration; $r1 ji$ and $r2 ji$ represent random numbers. It has been found that the less number of iterations is required to achieve optimum value of function as compared to genetic algorithm and particle swam optimization. It is also worthwhile to note here that there is not any requirement of population

size parameters unlike in genetic algorithm and particle swam optimization [25].

4 Results and Discussion

This section describes the outcomes obtained for CT and UAT processes. Response parameter surface roughness is discussed in first subsection. Chip breakability index is discussed in second subsection.

4.1 Surface Roughness

Figure 6a–c shows variation in surface roughness (R_a) with respect to speed in rpm at different feeds. In Table 4, surface roughness column shows the average value of R_a considering all three replicates. At a feed of 0.333 mm/rev, 12–17% improvement in R_a is obtained in the case of UAT process as compared to CT process for all rotational speed. At a feed 0.222 mm/rev, 11–22% improvement in R_a is observed at rotational speed 371 and 835 rpm, but at a rotational speed of 557 rpm no improvement is observed for UAT process as compared to CT process. The same trends are observed for feeds of 0.222 and 0.111 mm/rev in UAT process as compared to CT process. The results of the

analysis suggest that surface roughness is improved in UAT process in comparison with CT process. This improvement could primarily be attributed to a decrease in cutting zone temperature due to intermittent contact between tool and workpiece. Similar results are discussed by [12]. The decrease in temperature of the cutting tool causes low friction in the interface between flank and workpiece. This improves the surface finish of workpiece. Decreased temperature also results in lesser burr formation which results in the improved surface roughness of the workpiece [7].

4.2 Chip Breakability Index

Chip analysis is performed using the method described in the previous section. At a feed rate of 0.111 mm/rev, the chip is obtained mostly in the helical shape in both UAT and CT processes. At a feed rate of 0.222 mm/rev, arc shaped chip is obtained and at a feed rate of 0.333 mm/rev, ribbon shaped (frequently straight) chip is obtained in both UAT and CT processes. Better C_{in} is observed at a feed rate of 0.222 mm/rev as compared to a feed rate of 0.333 mm/rev and 0.111 mm/rev at all rotational speed and frequency. However, the chip breakability index is on the higher side (> 0.5) for all experiments due to blowholes
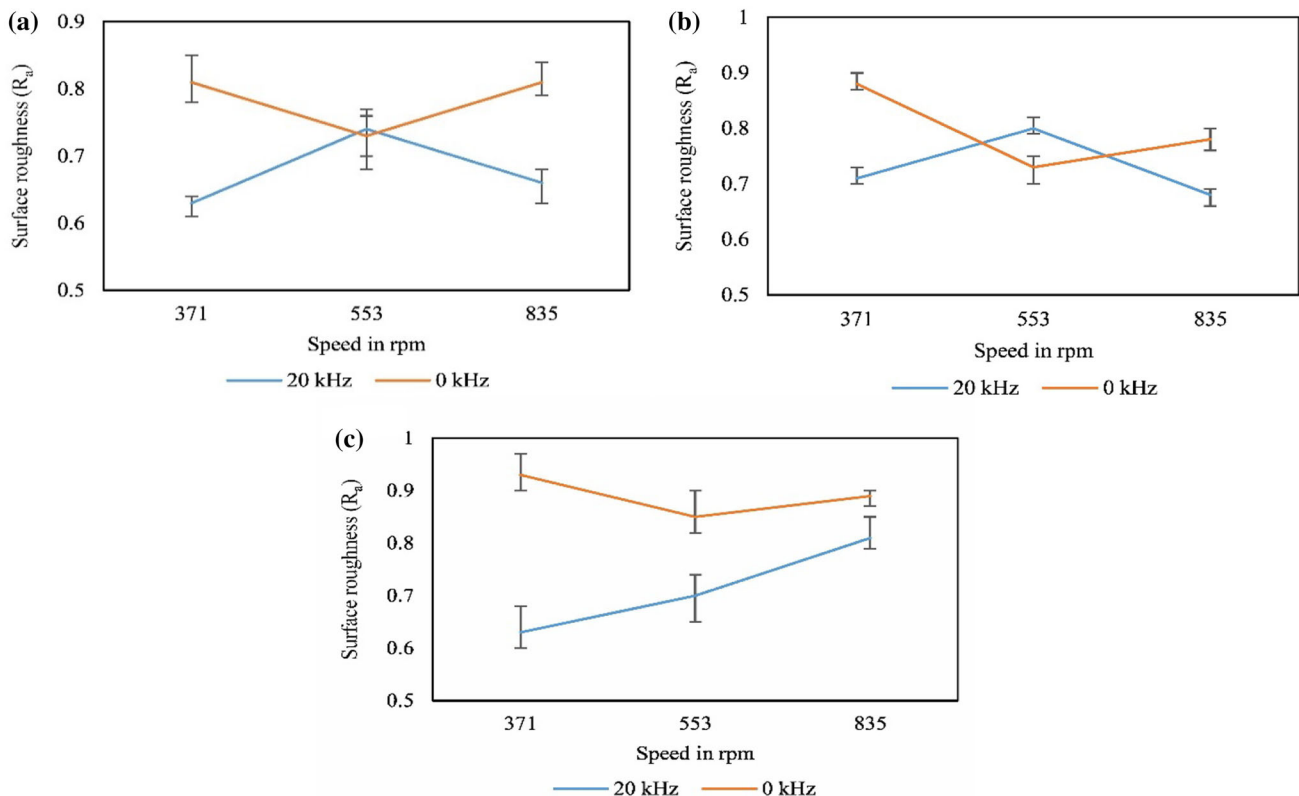

Fig. 6 Surface roughness variation with speed at feed of **a** 0.111 mm/rev, **b** 0.222 mm/rev and **c** 0.333 mm/rev
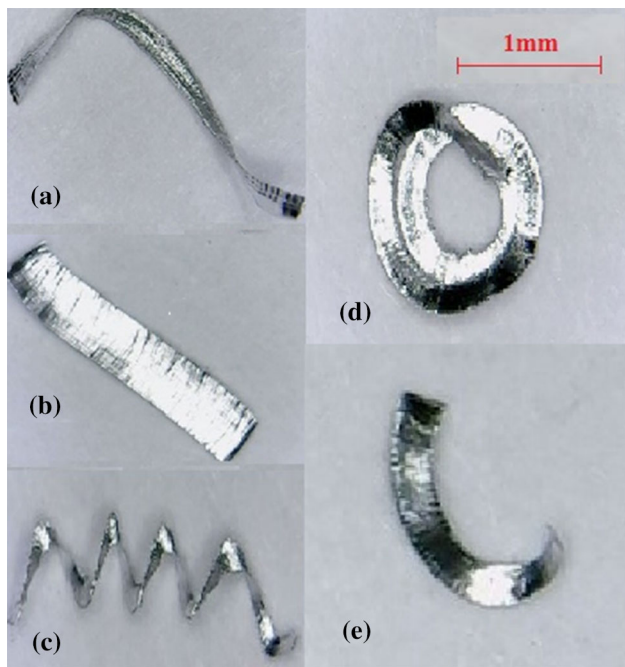
Fig. 7 Different chip shape **a** snarled, **b** straight, **c** helical, **d** spiral, **e** arc

and other defects present in in-house developed material. Figure 7a–e shows a different type of chips obtained during the experiment.

5 Modelling and Optimization

Equations (5) and (6) are regression models formulated for UAT and CT processes, respectively. Based on these regression equations, optimizations of surface roughness are performed using Jaya algorithm for UAT and CT processes separately. Response surfaces for UAT and CT processes using regression model are shown in Fig. 8a, b,
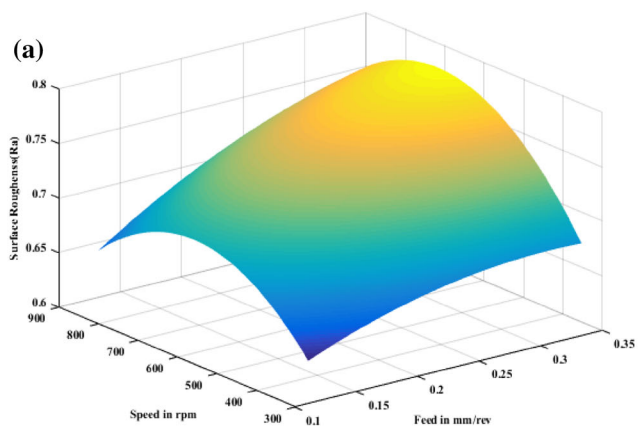
Table 5 Optimum parameters obtained for CT and UAT processes

Type of machining	N (rpm)	f (mm/rev)
CT	835	0.111
UAT	371	0.111

Table 6 Comparison of responses obtained from UAT and CUAT processes

Type of machining	N (rpm)	f (mm/rev)	F (kHz)	R_a (µm)	C_{in}	Types of chip produced
UAT	371	0.111	20	0.63	0.75	Helical
CUAT	371	0.111	20	0.40	0.83	Arc

respectively. Optimum parameters obtained for CT and UAT processes using Jaya algorithm are presented in Table 5.

$$
\begin{aligned}
R_a \, (\text{UAT}) &= (1.23955) - (0.000936 * N) - (1.68399 * f) \\
&\quad + \left(2.254518 * f^2\right) + (0.00197981 * f * N) \\
&\quad + \left(0.0000003178 * N^2\right)
\end{aligned}
\tag{5}
$$

$$
\begin{aligned}
R_a \, (\text{CT}) &= (0.379847) + (0.000879384 * N) \\
&\quad + (0.579919 * f) - \left(1.2039 * f^2\right) \\
&\quad + (0.000530016 * f * N) \\
&\quad + \left(0.0000007953 * N^2\right).
\end{aligned}
\tag{6}
$$

6 Hybrid Machining (CUAT)

The experiments are performed with CUAT process on optimum parameters of UAT process obtained from Table 5. For CUAT experiments, three replicates are recorded and average responses, namely R_a and C_{in}, are presented and compared in Table 6.
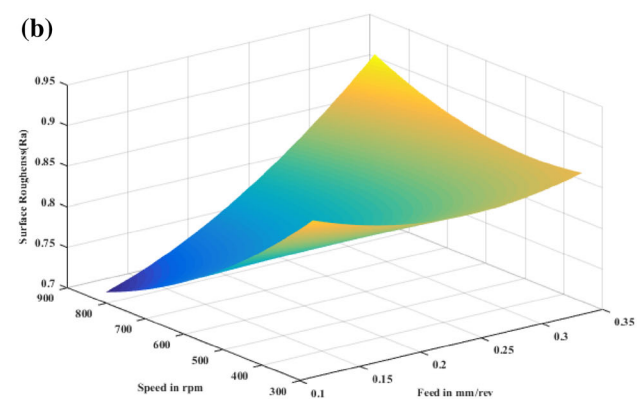

Fig. 8 Response surface **a** for UAT process and **b** for CT process

An improvement of 30–36.50% and 10–15% of surface roughness and C_{in} is found, respectively, in all three replicates recorded with CUAT process as compared with UAT process. Improvement of surface roughness is attributed to the capability of cryogenic fluid which drastically reduces the cutting zone temperature and maintains the shape of cutting edge. Improvement of chip breakability index is found due to embrittlement of chip at cryogenic temperature; similar results are discussed for Kevlar composites [26]. Another reason for better responses can be attributed to cryogenic fluid for making machining surfaces brittle [27], and UAT is suitable for machining of brittle surfaces as discussed by [8].

7 Conclusions

The surface roughness and chip breakability index during UAT and CT processes have been investigated using the regression analysis and Jaya algorithm. CUAT process is performed at optimum parameters obtained for UAT process. Cutting process parameters, namely rotational speed, feed and frequency, have been analysed. The subsequent conclusions can be listed from the above investigation:

- The UAT process is found to be better than CT process in respect of surface roughness for magnesium AZ91/SiC PMMC. However, the CUAT process outperforms the UAT process for achieving better surface roughness and chip breakability index.
- Optimization of regression models of surface roughness using Jaya algorithm reveals that the optimum cutting parameters for UAT and CT processes are as follows. The value of speed and feed is 835 rpm and 0.111 mm/rev, respectively, for CT process; 371 rpm and 0.111 mm/rev, respectively, for UAT process.
- The results of chip breakability indexes are comparable for both CT and UAT processes, but the better values of C_{in} are observed at a feed of 0.222 mm/rev for all rotational speed and frequency.
- An improvement up to 36.50% and 15% has been observed in surface roughness and chip breakability index, respectively, with CUAT process as compared to UAT process at optimized cutting parameters of the UAT process.

References

1. Watarai H, *Sci Technol Trends* **18** (2004) 84.
2. Pusavec F, Krajnik P, and Kopac J, *J Clean Prod* **18** (2010) 184.
3. Witte F, *Acta Biomater* **6** (2010) 1680.
4. Amini S, Nategh M J, and Soleimanimehr H, *Proc Inst Mech Eng Part B J Eng Manuf* **223** (2009) 641.
5. Pu Z, Outeiro J C, Batista A C, Dillon O W, Puleo D A, and Jawahir I S, *Procedia Eng* **19** (2011) 282.
6. Wang H, Estrin Y, Fu H, Song G, and Zúberová Z, *Adv Eng Mater* **9** (2007) 972.
7. Brehl D E and Dow T A, *Precis Eng* **32** (2008) 172.
8. Kulekci M K, *Int J Adv Manuf Technol* **39** (2008) 851.
9. Xu W X and Zhang L C, *Adv Manuf* **3** (2015) 173.
10. Kale A and Khanna N, *Procedia Manuf* **7** (2017) 191.
11. Shokrani A, Dhokia V, and Newman S T, *Proc Inst Mech Eng Part B J Eng Manuf* **232** (2018) 1690.
12. Babitsky V I, Mitrofanov A V, and Silberschmidt V V, *Ultrasonics* **42** (2004) 81.
13. Razfar M R, Sarvi P, and Zarchi M M A, *Proc Inst Mech Eng Part B J Eng Manuf* **225** (2011) 1615.
14. Pu Z, Outeiro J C, Batista A C, Dillon O W, Puleo D A, and Jawahir I S, *Int J Mach Tools Manuf* **56** (2012) 17.
15. Outeiro J C, Rossi F, Fromentin G, Poulachon G, Germain G, and Batista A C, *Procedia CIRP* **8** (2013) 487.
16. Danish M, Ginta T L, Habib K, Carou D, Rani A M A, and Saha B B, *Int J Adv Manuf Technol* **91** (2017) 2855.
17. Shen N, Ding H, Pu Z, Jawahir I S, and Jia T, *J Manuf Sci Eng* **139** (2017) 061012.
18. Di Iorio E, Bertolini R, Bruschi S, and Ghiotti A, *Procedia CIRP* **77** (2018) 324.
19. Abootorabi Zarchi M M, Razfar M R, and Abdullah A, *Proc Inst Mech Eng Part B J Eng Manuf* **226** (2012) 1185.
20. Khanna N, and Davim J P, *Meas. J Int Meas Confed* **61** (2015) 280.
21. Fang X D, Fei J and Jawahir I S, *Int J Mach Tools Manufact* **36** (1995) 1093.
22. Pusavec F, Deshpande A, Yang S, M'Saoubic R, Kopac J, and Jawahir I S, *J Clean Prod* **87** (2015) 941.
23. Hong J J, and W C Yeh, *Adv Mech Eng* **10** (2018) 1.
24. Rao R V, More K C, Oclon P, and Taler J, *Appl Therm Eng* **103** (2016) 572.
25. Rao R V, *Int J Ind Eng Comput* **7** (2016) 19.
26. Bhattacharyya D, Allen M N, and Mander S J, *Mater Manuf Process* **8** (1993) 631.
27. Iturbe A, Hormaetxe E, Garay A and Arrazola P J, *Procedia CIRP* **45** (2016) 67.